

# Hint of dark matter-dark energy interaction in the current cosmological data?

Vidhya Ganesan,<sup>1,\*</sup> Amlan Chakraborty,<sup>1,†</sup> Tulip Ray,<sup>2,‡</sup> Subinoy Das,<sup>1,§</sup> and Arka Banerjee<sup>3,¶</sup>

<sup>1</sup>*Indian Institute of Astrophysics, Bengaluru, Karnataka 560034, India*

<sup>2</sup>*Department of Physics, Indian Institute of Technology Kharagpur, Kharagpur 721302, India*

<sup>3</sup>*Department of Physics, Indian Institute of Science Education and Research,  
Homi Bhabha Road, Pashan, Pune 411008, India*

Many previous studies have explored models of dynamically interacting dark energy scenarios instead of a cosmological constant and cold dark matter. This work aims to offer a comprehensive investigation of the Yukawa-type interaction between dark energy and dark matter where dark matter mass is also a function of a dynamical scalar field value. Unlike previous work, instead of taking an approximate solution, we numerically solve the Klein-Gordon equation that governs the intricate interplay between these two components of the dark sector along with the corresponding perturbations, using a suitable shooting algorithm to determine precise initial conditions. We have conducted a thorough analysis of this interaction using the Markov Chain Monte Carlo method, incorporating diverse datasets such as Planck, BAO, Pantheon+, and SH<sub>0</sub>ES. Our results, for the first time, reveal a discernible detection of the coupling constant, which encapsulates the strength of the dark sector interaction. We find non-zero  $\beta$  values of 0.0487, 0.0680, 0.0712, and 0.0822 (68% Confidence Limit) corresponding to the inclusion of each dataset, respectively. Notably, the addition of SH<sub>0</sub>ES data led to a significant increase in the prominence of  $\beta$ , suggesting the potential for new physics in the dark sector. This study serves as a strategic road map for future endeavours with non-linear cosmology, which will contribute to an enhanced understanding and refinement of constraints on the dark sector interaction.

## I. INTRODUCTION

The standard six-parameter phenomenological  $\Lambda$ CDM model has been successful in explaining the evolution of the Universe, both for the smooth background, as well as for fluctuations at linear scales [1–5]. However, recent precision observations have revealed several anomalies, such as the “Hubble tension” and the “ $S_8$  tension” [6, 7]. On the theoretical front, the smallness of cosmological constant ( $\Lambda$ ) has remained a challenge for fundamental particle physics [8]. While current observations are mostly consistent with dark energy being a cosmological constant, cosmological measurements have thus far been unable to offer any insights about its origin or smallness.

The existence of dynamic dark energy has been explored as an alternative possibility where the equation of state of dark energy is time dependant [9–12], which results in a unique imprint on the growth of structures in the universe. Such models can be probed through their imprints in existing and upcoming cosmological observations. In this regard, an even more interesting possibility could be interactions in the dark sector, for instance, between dark energy and dark matter [13, 14], which could potentially leave signatures on various cosmological observables. In fact, in the absence of any symmetry forbidding such an interaction, the scalar field dark energy interacting with dark matter fermion can occur in

nature [13]. Consequently, several scalar-tensor theories have been proposed in the literature to model interacting dark energy and dark matter [15–71].

The Chameleon dark energy model [27], is one such prominent model that exhibits an interesting feature of dark energy equation of state parameter  $w < -1$  without violating the weak energy principle or cosmic catastrophe [72–74]. This model is predominantly parameterised by two parameters, namely the slope of the potential  $\alpha$  and the interaction strength  $\beta$  between dark matter and dark energy, which have their origin in string theory of compactification [75]. This paper presents a detailed investigation of the Chameleon dark energy model. Unlike the previous work in Boriero et. al. [76]<sup>1</sup>, here we have numerically solved the Klein-Gordon equation (modified form for Chameleon model shown in Eq. 1) by deploying a shooting algorithm to evaluate the initial condition of the scalar field. The analysis demonstrates that this model is consistent with cosmological data. Moreover, a peak feature is observed in  $\beta$  for the first time, indicating a mild detection of the fifth force. It is interesting to note that the previous studies have only put an upper limit on the  $\beta$  value. Perhaps the exact numerical solution adopted in this work and the use of recent data sets for the analysis could have led to this slight detection of fifth force in the dark sector. If this is true, the inclusion of non-linear scales in our future analysis will open up new avenues to probe fifth force. Specifically, its imprint on the highly precise measurements from various stage IV cosmological surveys in the next decade will provide much more insight into either ruling out or detecting such a fifth force with more significance. We can also expect a unique signature of non-zero  $\beta$  value on the difference in infall between the dark matter and baryonic matter,

\* [vidhya.gnsn@gmail.com](mailto:vidhya.gnsn@gmail.com)

† [amlan.chakraborty@iiap.res.in](mailto:amlan.chakraborty@iiap.res.in)

‡ [tulipray2804@gmail.com](mailto:tulipray2804@gmail.com)

§ [subinoy@iiap.res.in](mailto:subinoy@iiap.res.in)

¶ [arka@iiserpune.ac.in](mailto:arka@iiserpune.ac.in)

into the virialised halos [77–79]. These effects will be accurately studied with N-body simulations in our future work.

The plan of the paper is as follows. In section II, we briefly describe the chameleon model and its effect on background cosmology as well as perturbations. In section III, we discuss the possible impact of dark sector interaction on various cosmological probes. In section IV, we elaborate on the numerical implementation of this model and present the result from our MCMC analysis with different datasets. We conclude in section V.

## II. THE CHAMELEON MODEL

This work endeavours to thoroughly study the Yukawa-type interaction between dark energy and dark matter. We adopt a popular Chameleon-type model, which represents dark energy as a scalar field whose mass depends on local dark matter density [27–29, 80–82]. In our case, to circumvent the stringent constraints imposed by the solar system tests of gravity on Chameleon models [83, 84], we assume that the dark energy only interacts with dark matter and does not have any interaction with the visible sector [74, 82].

### 1. Background evolution

The dark energy is modeled as a scalar field,  $\phi$ , coupled to dark matter as  $f(\phi)\bar{\psi}\psi$ , where  $f(\phi)$  is an arbitrary function of  $\phi$  and  $\psi$  is the dark matter Dirac spinor. The Klein-Gordon equation governing the dynamics of this scalar field (obtained by minimizing the action describing the Chameleon scalar field [29]) is given by

$$\ddot{\phi} + 3H\dot{\phi} = -V_{,\phi}(\phi) - \frac{\rho_{DM}^{(0)}}{a^3} \frac{f_{,\phi}(\phi)}{f(\phi_0)}. \quad (1)$$

The “dot” in the equation represents differentiation with respect to cosmic time, while  $\phi_0$  and  $\rho_{DM}^{(0)}$  denote the present-day scalar field and dark matter density, respectively. The scalar field experiences an effective potential

$$V_{\text{eff}}(\phi) = V(\phi) + \frac{\rho_{DM}^{(0)}}{a^3} e^{\beta(\phi-\phi_0)/M_{Pl}}, \quad (2)$$

where the coupling function is taken as  $f(\phi) = e^{\beta\phi/M_{Pl}}$ , where  $M_{Pl} \equiv (8\pi G)^{-1/2}$  is the reduced Planck mass. Such exponential form emerges from string theory models of compactification [75].

We consider the self-interaction potential to be a simple power law runaway type,

$$V(\phi) = M_\phi^4 \left( \frac{M_{Pl}}{\phi} \right)^\alpha. \quad (3)$$

The slope of the potential is described by a positive constant, denoted by  $\alpha$ .  $M_\phi \approx \left[ \rho_\phi^{(0)} \left( \frac{\phi_0}{M_{Pl}} \right)^\alpha \right]^{1/4}$  is the scalar field mass.

In the limit of vanishing coupling parameter  $\beta$  with constant potential  $V(\phi)$  and constant scalar field, the model reduces to the standard  $\Lambda$ CDM model.

Furthermore, the dark matter and dark energy density for this model, are given by

$$\rho_{DM} = \frac{\rho_{DM}^{(0)}}{a^3} e^{\beta(\phi-\phi_0)/M_{Pl}}, \quad \rho_{DE} = \rho_\phi = \frac{1}{2}\dot{\phi}^2 + V(\phi). \quad (4)$$

An interesting aspect of this model, as shown in the work [74], is that an observer unaware of the existence of dark sector interaction would end up estimating an equation of state (EoS) different from the actual value,  $w_\phi = P_\phi/\rho_\phi$ . The observed EoS will become

$$w_{obs} = \frac{w_\phi}{1-x}, \quad \text{where } x = \frac{\rho_{DM}^{(0)}}{a^3 \rho_\phi} [e^{\beta(\phi-\phi_0)/M_{Pl}} - 1].$$

Specifically, it was shown that even though the actual Chameleon dark energy does not have any phantom behaviour, the observer ends up noting an apparent phantom behaviour. This may explain the slight phantom EoS observed in several independent probes such as [85–87], indirectly indicating the presence of dark sector interaction.

### 2. Evolution of inhomogeneities

The coupling in the dark sector leads to modification in the evolution of inhomogeneities in the Universe.

In the synchronous gauge, the equations of motion for the dark matter density contrast  $\delta_{DM}(k, t)$ , velocity divergence  $\theta_{DM}(k, t)$  and scalar field perturbations [88] for a Fourier mode  $k$  are given by

$$\begin{aligned} \dot{\delta}_{DM} &= - \left( \frac{\theta_{DM}}{a} + \frac{\dot{\tilde{h}}}{2} \right) + \frac{\beta}{M_{Pl}} \delta\dot{\phi}, \\ \dot{\theta}_{DM} &= -H\theta_{DM} + \frac{\beta}{M_{Pl}} \left( \frac{k^2}{a} \delta\phi - \dot{\phi}\theta_{DM} \right), \\ \delta\ddot{\phi} + 3H\delta\dot{\phi} + \left( \frac{k^2}{a^2} + V_{,\phi\phi} \right) \delta\phi + \frac{1}{2}\dot{\tilde{h}}\dot{\phi} &= -\frac{\beta}{M_{Pl}} \rho_{DM} \delta_{DM} \end{aligned} \quad (5)$$

where  $\tilde{h} \equiv \tilde{h}_i^i$  is the trace of metric perturbation  $\tilde{h}_{ij}$ , obtained from perturbed Einstein equation.

<sup>1</sup> In Boriero et. al. [76], an approximate analytical solution of the modified Klein-Gordon equation (refer Eq. 1) was used for the analysis while in the current work we use the exact solution obtained by numerically solving it using the shooting method.

### III. IMPACT OF DARK SECTOR INTERACTION ON THE COSMOLOGICAL PROBES

In the standard cosmological framework, the dark sector of the Universe can only be detected and studied through their gravitational effects. Any detection of  $w_{DE} \neq -1$  can be interpreted as a departure from the standard cosmological constant, without any implications for dark matter. This comes under  $w$ CDM paradigm, where the energy densities of dark energy and dark matter are treated as background quantities with separate (uncoupled) evolution equations.

When we consider models with dark sector interaction, it leads to degeneracy between the features induced due to the presence of dark sector interaction and those from the standard cosmological parameters. Specifically, the dark sector coupling uniquely modifies the evolution of matter/radiation perturbations and hence also the clustering properties of galaxies. In order to test a dark sector interaction model, one needs to identify these unique features on the evolving density perturbations in the linear and non-linear phases using the latest data. Here in this subsection, we note some of the consequences of Chameleon dark sector interaction on the cosmological probes.

The ratio of dark matter density in the Chameleon model to the corresponding dark matter density in  $\Lambda$ CDM model has to be small otherwise it leads to conflicts with the observational estimates of matter density at various redshifts such as galaxy counts, weak lensing etc [89]. Hence in order for the Chameleon dark matter to be consistent with these observations it needs to behave as a normal dark matter for most of the cosmological history except in the later times. This requires that the self interacting scalar field potential in Eq. 3 to be sufficiently flat i.e.  $\alpha \lesssim 0.2$  [74]. In our current work, we set the value of  $\alpha$  as 0.01, satisfying this condition as well as increasing the computational efficiency for the analysis in the subsequent section.

The evolution equation for dark matter inhomogeneities in synchronous gauge with slow roll approximation is given by [90]

$$\ddot{\delta}_{DM} + 2H\dot{\delta}_{DM} = \frac{3}{2}H^2 \left( 1 + \frac{2\beta^2}{1 + a^2 V_{,\phi\phi}/k^2} \right) \delta_{DM}. \quad (6)$$

This equation differs from the corresponding expression for  $\Lambda$ CDM by the factor inside the brackets. The extra term proportional to  $\beta^2$  arises due to the fifth force mediated by the scalar field. The comoving finite range of this force, for the potential form in Eq. 3, is given by

$$\lambda_c = a^{-1} V_{,\phi\phi}^{-1/2} \approx a^2 H_0^{-1} \sqrt{\frac{\Omega_\phi}{\Omega_{DM}^2} \frac{\alpha}{3\beta^2}} e^{-\beta(\phi-\phi_0)/M_{Pl}}, \quad (7)$$

where  $\alpha \ll 1$ . The perturbations whose physical scale are much larger than  $\lambda_c$  i.e.  $a/k \gg \lambda_c$  evolves similar to

that in the  $\Lambda$ CDM model. However, perturbations with smaller comoving scales evolves such that the Newton's constant is modified by a factor of  $(1 + 2\beta^2)$ . Thus the existence of dark sector interactions results in an extra attractive force between the dark matter particles which leads to enhancement of power on small scales and also enhances the growth of perturbations. Hence these small scale perturbations becomes non-linear earlier than those in the  $\Lambda$ CDM model.

Furthermore, it can be noted from the Eq. 7 that the fifth force range,  $\lambda_c$ , today is comparable to the Hubble length today. While at earlier times the Chameleon interaction range was suppressed due to the scale factor. For example at the time of CMB decoupling, the Chameleon force range was much smaller than the Hubble horizon at the time. Hence we can conclude that the presence of Chameleon dark sector interaction will not effect the CMB primary anisotropy.

### IV. DETECTING AND CONSTRAINING THE DARK SECTOR INTERACTION STRENGTH

#### A. Numerical method: Solving the Background and Perturbation equations using the Shooting Algorithm

We have modified the publicly available CLASS [91, 92] to solve the background and perturbation equations of the Chameleon model (Eqs. 1, 5 together with the Friedmann and perturbed Einstein equation). In order to get the correct dark energy density today,  $\rho_{DE}^{(0)}$ , we use the shooting feature inbuilt in CLASS to set the initial scalar field value,  $\phi_i$ , such that the current dark energy density value matches its observational value today. This is similar to what we do in the case of standard  $\Lambda$ CDM model, where we set the value of cosmological constant,  $\Lambda$ , such that its value matches the local dark energy density. Specifically, we first choose a  $\phi_i$  value, evolve the background equations and then we estimate the current dark energy density. We keep repeating this process by varying the  $\phi_i$  value until we find a value which finally gives the correct local dark energy density.

The CMB power spectrum of temperature and E mode, and the matter power spectrum obtained are shown in the top panels of the Fig. 1 respectively, for the Chameleon model (blue) and  $\Lambda$ CDM model (red). The fractional difference of the Chameleon model with respect to  $\Lambda$ CDM model corresponding to each of these power spectrum are shown in the bottom panels. The Planck 2018 power spectrum error-bars [93] for the CMB temperature and E mode are also shown in the respective panels.

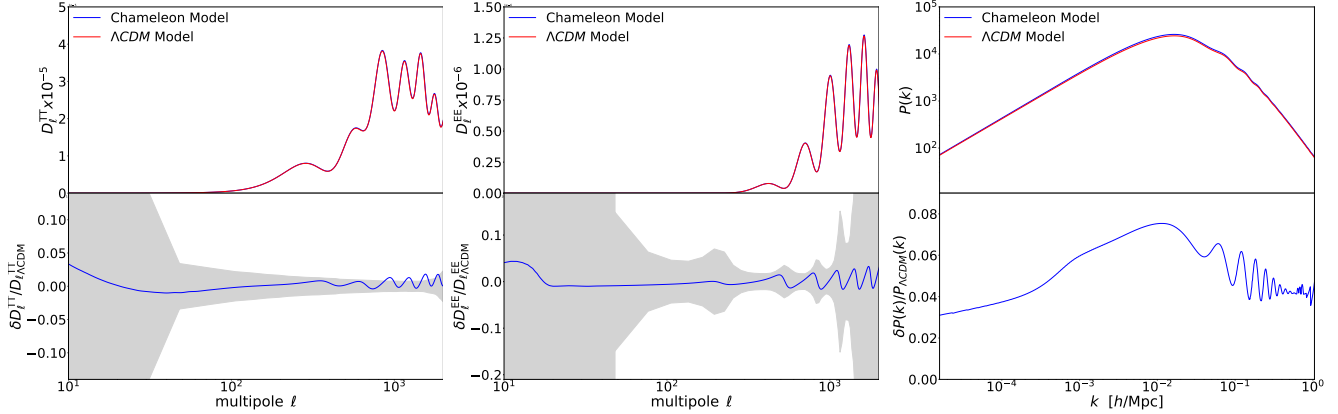


FIG. 1. The top panels show the power spectrum for the CMB temperature (left) and E mode (middle), and also the matter power spectrum (right), for  $\Lambda$ CDM model (red) and Chameleon model (blue) with  $(\alpha, \beta) = (0.01, 0.1)$ . The bottom panels shows the fractional difference in these power spectra for the Chameleon model with respect to the  $\Lambda$ CDM model. The Planck 2018 power spectrum error bars corresponding to the CMB temperature and E mode are also shown in the respective panels.

Dataset	Planck		Planck + BAO	
	$\Lambda$ CDM	Chameleon	$\Lambda$ CDM	Chameleon
$100\omega_b$	2.2352(2.2489) $^{+0.01525}_{-0.01552}$	2.2430(2.2500) $^{+0.01655}_{-0.01736}$	2.2415(2.2442) $^{+0.01399}_{-0.01371}$	2.2491(2.2570) $^{+0.01505}_{-0.01590}$
$\omega_{dm}$	0.1202(0.1194) $^{+0.00141}_{-0.00142}$	0.1230(0.1224) $^{+0.00133}_{-0.00131}$	0.1193(0.1195) $^{+0.00102}_{-0.00103}$	0.1222(0.1214) $^{+0.00098}_{-0.00098}$
$100\theta_s$	1.0419(1.0419) $^{+0.00030}_{-0.00030}$	1.0419(1.0418) $^{+0.00030}_{-0.00029}$	1.0420(1.0421) $^{+0.00028}_{-0.00028}$	1.0419(1.0419) $^{+0.00028}_{-0.00028}$
$\log(10^{10} A_s)$	3.0455(3.0378) $^{+0.01568}_{-0.01676}$	3.0429(3.0448) $^{+0.01556}_{-0.01632}$	3.0462(3.0415) $^{+0.01559}_{-0.01731}$	3.0431(3.0513) $^{+0.01607}_{-0.01653}$
$n_s$	0.9647(0.9663) $^{+0.00450}_{-0.00458}$	0.9649(0.9637) $^{+0.00447}_{-0.00456}$	0.9669(0.9644) $^{+0.00389}_{-0.00388}$	0.9669(0.9687) $^{+0.00388}_{-0.00395}$
$\tau_{reio}$	0.0545(0.0521) $^{+0.00763}_{-0.00820}$	0.0533(0.0548) $^{+0.00758}_{-0.00796}$	0.0557(0.0524) $^{+0.00740}_{-0.00829}$	0.0543(0.0595) $^{+0.00760}_{-0.00799}$
$\beta$	—	0.0512(0.0487) $^{+0.03253}_{-0.02785}$	—	0.0537(0.0680) $^{+0.03372}_{-0.02712}$
$H_0$	67.3000(67.6870) $^{+0.62469}_{-0.63540}$	67.6770(67.9310) $^{+0.62567}_{-0.65097}$	67.6990(67.6710) $^{+0.44644}_{-0.47054}$	68.0350(68.4270) $^{+0.47362}_{-0.48113}$
$\sigma_8$	0.8114(0.8059) $^{+0.00771}_{-0.00763}$	0.8233(0.8178) $^{+0.00978}_{-0.01368}$	0.8092(0.8074) $^{+0.00700}_{-0.00764}$	0.8222(0.8261) $^{+0.01024}_{-0.01402}$
$\chi^2_{min}$	2771.7913	2771.1117	2777.0758	2776.0405
$\Delta\chi^2_{min}$	0	-0.6796	0	-1.0353

TABLE I. The mean (bestfit)  $\pm 1\sigma$  error for the cosmological parameters constrained with the datasets [Planck] and [Planck + BAO] for the  $\Lambda$ CDM model and Chameleon model are shown in the above table. The corresponding  $\chi^2_{min}$  and  $\Delta\chi^2_{min}$  values are also shown.

## B. Details of the MCMC Analysis

### 1. Data sets

We use a combination of Cosmic Microwave Background [CMB], Baryon Acoustic Oscillation [BAO], Pantheon+ and SH<sub>0</sub>ES datasets. The details of these datasets are as follows:

- Planck 2018 measurements of the high- $\ell$  CMB TT, TE, EE, and low- $\ell$  CMB TT, EE power spectra [1].
- The BAO measurements from SDSS-III Baryon Oscillation Spectroscopic Survey DR12 galaxy sample at the redshifts  $z = 0.38, 0.51$  and  $0.61$  [94], 6dF Galaxy Survey (6dFGS) at  $z = 0.106$  [95], and SDSS DR7 Main Galaxy Sample I at  $z = 0.15$  [96].

- Pantheon+ data with Type Ia supernovae (SNe Ia) catalogue ranging in redshifts from  $z = 0.001$  to  $2.26$  [97].
- SH<sub>0</sub>ES data with Cepheids variables in the host galaxies with nearby or recent SNe Ia discovered in the last four decades with  $z \leq 0.01$  [98].

### 2. Methodology

We consider the baseline cosmology to consist of six  $\Lambda$ CDM parameters [ $\omega_b, \omega_{dm}, \theta_s, \ln(10^{10} A_s), n_s, \tau_{reio}$ ] plus the two Chameleon model parameters  $\alpha$  and  $\beta$ .

In this study, we perform a Markov Chain Monte Carlo (MCMC) analysis using the publicly available package

Dataset	Planck + BAO + Pantheon+		Planck + BAO + Pantheon+ + SH <sub>0</sub> ES	
Model	$\Lambda$ CDM	Chameleon	$\Lambda$ CDM	Chameleon
$100\omega_b$	2.2385(2.2421) <sup>+0.01382</sup> <sub>-0.01337</sub>	2.2452(2.2501) <sup>+0.01409</sup> <sub>-0.01605</sub>	2.2606(2.2475) <sup>+0.01351</sup> <sub>-0.01323</sub>	2.2699(2.2845) <sup>+0.01483</sup> <sub>-0.01579</sub>
$\omega_{dm}$	0.1197(0.1188) <sup>+0.00095</sup> <sub>-0.00097</sub>	0.1227(0.1231) <sup>+0.00091</sup> <sub>-0.00094</sub>	0.1174(0.1171) <sup>+0.00088</sup> <sub>-0.00086</sub>	0.1206(0.1202) <sup>+0.00083</sup> <sub>-0.00086</sub>
$100\theta_s$	1.0419(1.0418) <sup>+0.00030</sup> <sub>-0.00026</sub>	1.0419(1.0418) <sup>+0.00028</sup> <sub>-0.00030</sub>	1.0422(1.0420) <sup>+0.00028</sup> <sub>-0.00027</sub>	1.0421(1.0419) <sup>+0.00029</sup> <sub>-0.00028</sub>
$\log(10^{10} A_s)$	3.0459(3.0354) <sup>+0.01548</sup> <sub>-0.01607</sub>	3.0430(3.0566) <sup>+0.01575</sup> <sub>-0.01695</sub>	3.0485(3.0451) <sup>+0.01642</sup> <sub>-0.01804</sub>	3.0444(3.0423) <sup>+0.01621</sup> <sub>-0.01730</sub>
$n_s$	0.9659(0.9650) <sup>+0.00363</sup> <sub>-0.00379</sub>	0.9657(0.9661) <sup>+0.00397</sup> <sub>-0.00368</sub>	0.9716(0.9726) <sup>+0.00374</sup> <sub>-0.00364</sub>	0.9714(0.9742) <sup>+0.00373</sup> <sub>-0.00373</sub>
$\tau_{reio}$	0.0552(0.0513) <sup>+0.00750</sup> <sub>-0.00776</sub>	0.0538(0.0576) <sup>+0.00752</sup> <sub>-0.00799</sub>	0.0589(0.0574) <sup>+0.00752</sup> <sub>-0.00903</sub>	0.0568(0.0565) <sup>+0.00756</sup> <sub>-0.00841</sub>
$\beta$	—	0.0520(0.0712) <sup>+0.03204</sup> <sub>-0.02781</sub>	—	0.0660(0.0822) <sup>+0.03519</sup> <sub>-0.02168</sub>
$H_0$	67.5210(67.8240) <sup>+0.42498</sup> <sub>-0.43026</sub>	67.8220(67.6550) <sup>+0.43965</sup> <sub>-0.46707</sub>	68.6160(68.5760) <sup>+0.38578</sup> <sub>-0.39766</sub>	68.9440(69.1480) <sup>+0.42046</sup> <sub>-0.41728</sub>
$\sigma_8$	0.8102(0.8026) <sup>+0.00726</sup> <sub>-0.00689</sub>	0.8228(0.8358) <sup>+0.00966</sup> <sub>-0.01354</sub>	0.8045(0.8027) <sup>+0.00727</sup> <sub>-0.00778</sub>	0.8224(0.8258) <sup>+0.01147</sup> <sub>-0.01598</sub>
$\chi^2_{min}$	4189.5447	4189.3447	4104.1945	4101.2884
$\Delta\chi^2_{min}$	0	-0.2000	0	-2.9061

TABLE II. The mean (bestfit)  $\pm 1\sigma$  error for the cosmological parameters constrained with the datasets [Planck + BAO + Pantheon Plus] and [Planck + BAO + Pantheon Plus + SH<sub>0</sub>ES] for the  $\Lambda$ CDM model and Chameleon model are shown in the above table. The corresponding  $\chi^2_{min}$  and  $\Delta\chi^2_{min}$  values are also shown.

MontePython-v3 [99], which implements the Metropolis Hasting algorithm. This is then interfaced with CLASS modified for the Chameleon model with the datasets mentioned in the previous subsection. We use Cholesky decomposition, which efficiently samples the fast and slow parameters to cover the entire parameter space [100]. We consider the chains to be converged when the Gelman-Rubin convergence criterion,  $R - 1 < 0.01$ , is met [101]. Finally, we obtain the minimized  $\chi^2$  using the Sequential Least Squares Programming algorithm built into the Montepython code.

### C. Results

In this work, our main focus is on the dark sector interaction strength from different cosmological datasets. In order to obtain an estimate for the strength of Chameleon interaction,  $\beta$ , we fix  $\alpha = 0.01$  as discussed in Sec. III. The mean and best fit values of the parameters obtained from the MCMC runs are shown in Tables I and II. The Table I shows the values for the datasets Planck, and Planck + BAO. While the Table II shows for the datasets Planck + BAO + Pantheon Plus, and Planck + BAO + Pantheon Plus + SH<sub>0</sub>ES. The  $\chi^2_{min}$  and  $\Delta\chi^2_{min}$  values obtained for different datasets are also shown in tables. The  $\chi^2_{min}$  for each experiment are reported in Appendix A. The plots of 1D and 2D posterior distribution of  $\beta, \omega_{dm}, H_0$  and  $\sigma_8$  are shown in the Fig. 2. This figure shows the comparison of Chameleon model between different datasets namely: Planck, Planck + BAO, Planck + BAO + Pantheon Plus, and Planck + BAO + Pantheon Plus + SH<sub>0</sub>ES.

The strength of dark sector interaction,  $\beta$ , indicated by the mean value of its posterior distribution from MCMC runs using different dataset combinations of Planck, BAO, Pantheon Plus, and SH<sub>0</sub>ES are found to be about 0.0512, 0.0537, 0.0520, 0.0660 in tandem with the inclusion of each dataset respectively. The corresponding bestfit values are 0.0487, 0.0680, 0.0712, 0.0822 respectively. Further, the

corresponding  $\Delta\chi^2_{min}$  for the Chameleon model with respect to the  $\Lambda$ CDM model comes out to be about  $-0.6796, -1.0353, -0.2000, -2.9061$  respectively. The lowest  $\Delta\chi^2$  corresponds to the Planck + BAO + Pantheon Plus + SH<sub>0</sub>ES dataset while the highest  $\Delta\chi^2$  corresponds to the Planck + BAO + Pantheon Plus dataset. Even though these  $\Delta\chi^2$  values does not indicate a very significant preference but still all of the different dataset combinations show a slight preference to the Chameleon model over the standard  $\Lambda$ CDM model.

Further, we note that the Chameleon model results in higher mean values of  $H_0, \sigma_8$  and  $\omega_{dm}$  in comparison to the  $\Lambda$ CDM model as shown in the Tables I and II.

Here, we list the interesting features noted in the 1D posterior distribution of  $\beta$  in Fig. 2, which are as follows:

- ▶ The posterior distribution corresponding to all of the different dataset combinations shows a peak with upper bound but no lower bound.
- ▶ The addition of BAO dataset to the Planck dataset leads to a slight decrease in the likelihood value at  $\beta = 0$ .
- ▶ Further, the addition of Pantheon Plus dataset leads to a smoother drop in the likelihood value near  $\beta = 0$  other than this it does not significantly alter the shape in comparison to the previous case.
- ▶ Finally with the addition of SH<sub>0</sub>ES dataset, we see a dramatic improvement as the likelihood value at  $\beta = 0$  decreases significantly. The mean value also shifts significantly in comparison to the above cases.
- ▶ The consecutive addition of BAO, Pantheon Plus and SH<sub>0</sub>ES datasets to the Planck dataset, decreases the likelihood value at  $\beta = 0$ .
- ▶ All of the different dataset combinations show a higher likelihood value at the non-zero mean  $\beta$  value in comparison to the likelihood value at  $\beta = 0$ .



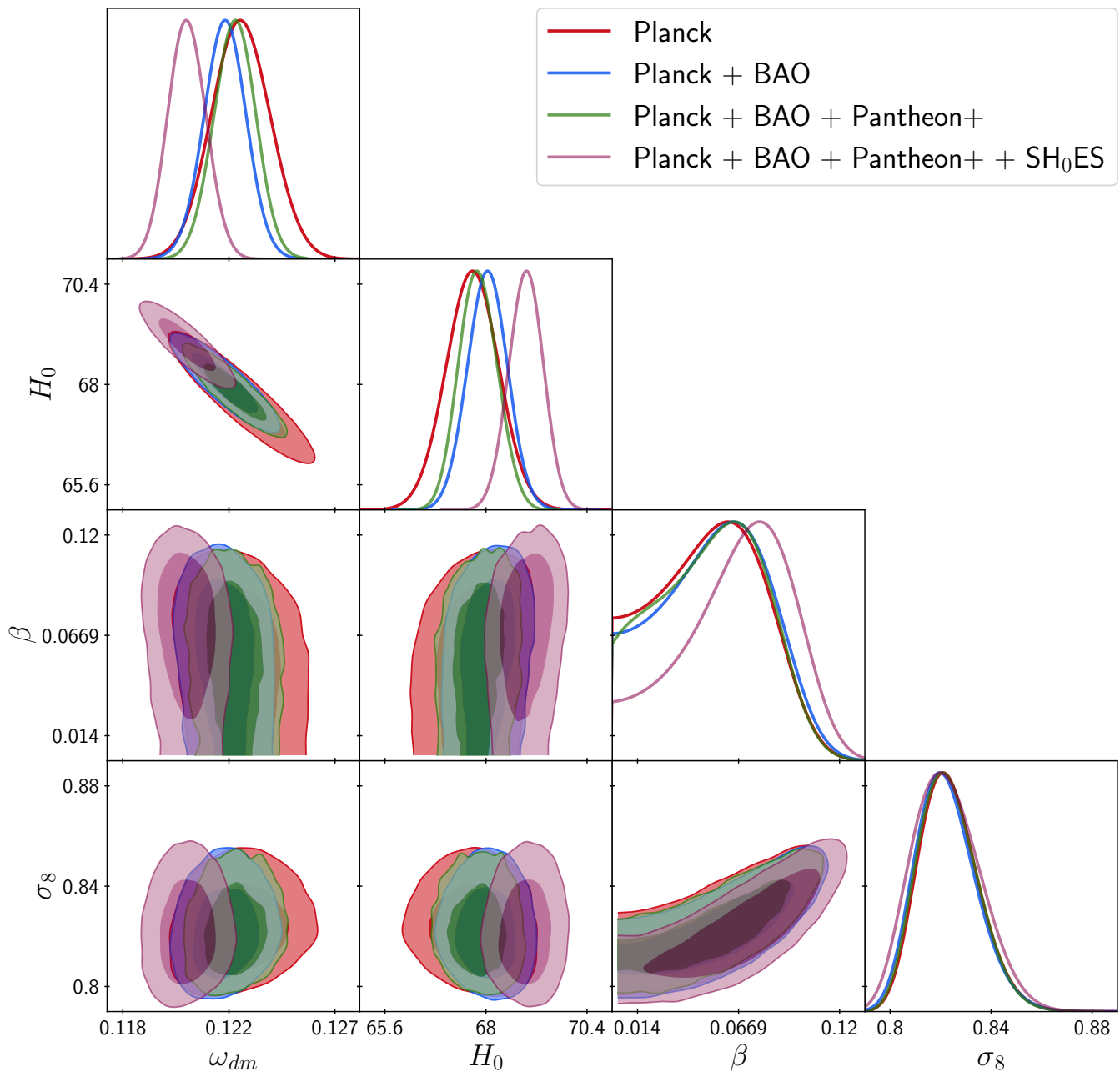


FIG. 2. Posterior distribution for the Chameleon model with different datasets.

The last point implies that all of the different dataset combinations consistently show a preference for non-zero  $\beta$  value rather than for  $\beta = 0$  (which refers to non-interacting dark sector). This clearly implies that the cosmological datasets are hinting at a more versatile interacting dark sector.

The 2D posterior distribution of  $\beta$  with other parameters show features similar to those of 1D posterior distribution and hence a similar conclusion can be drawn.

The above MCMC analysis was also implemented with different  $\alpha$  values such as 0.005, 0.05 and 0.1. The 1D and 2D posterior distributions obtained with the Planck +

BAO + Pantheon Plus + SH<sub>0</sub>ES dataset corresponding to each of these  $\alpha$  values are shown in Fig. 3. The inferences that can be drawn from the posterior distributions of  $\beta$  are listed as follows:

- The posterior distributions corresponding to all of the different  $\alpha$  value shows a peak with an upper bound but no lower bound.
- Posterior distributions corresponding to all of the different  $\alpha$  values consistently show a higher likelihood value at a non-zero mean  $\beta$  value in comparison to the likelihood value at  $\beta = 0$ . This indicates

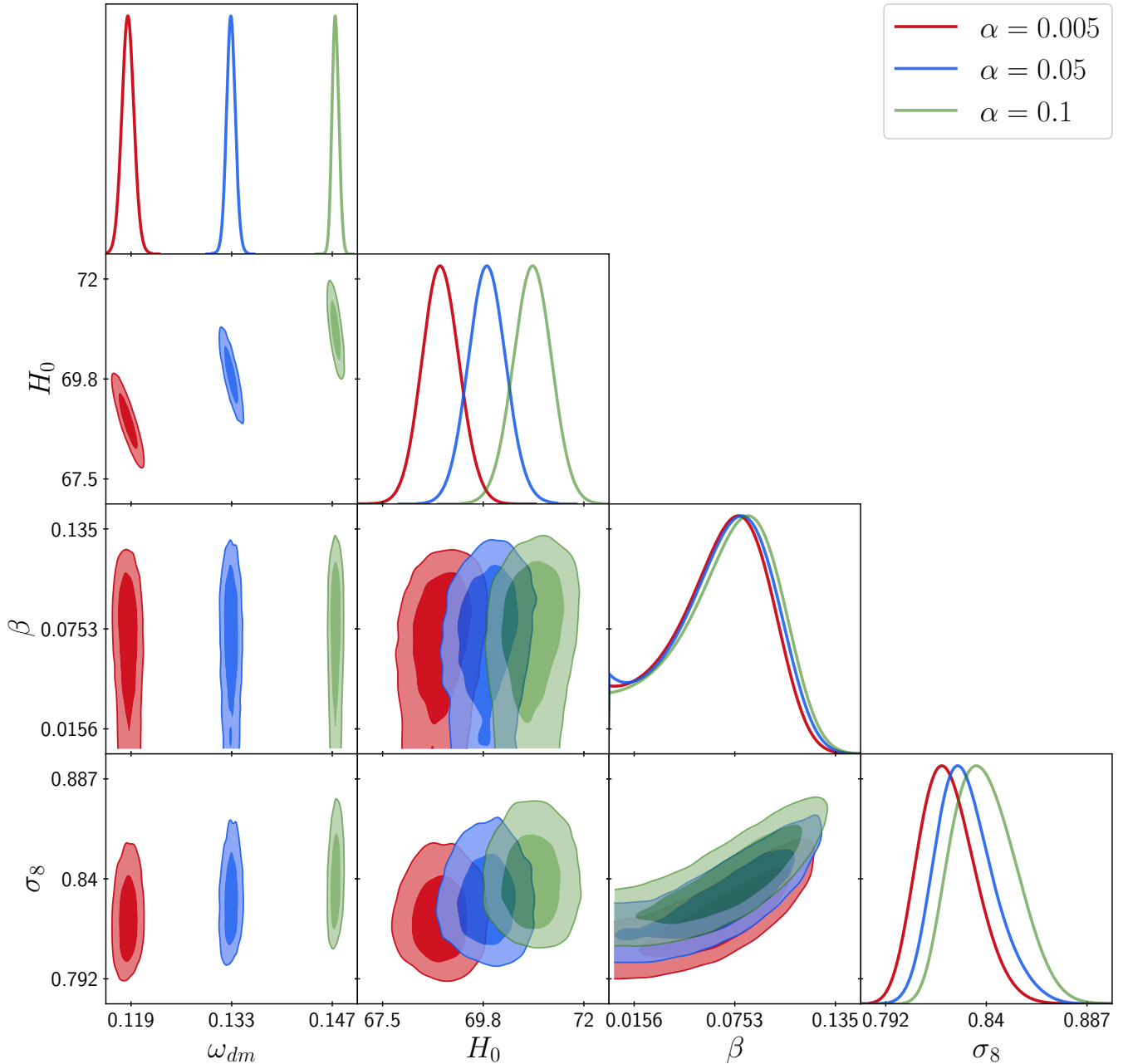


FIG. 3. Posterior distribution for the Chameleon model with Planck + BAO + Pantheon Plus + SH<sub>0</sub>ES dataset for the  $\alpha$  values 0.005, 0.05, and 0.1.

a preference for a non-zero  $\beta$  value rather than for  $\beta = 0$  case.

- The peak position seems to remain robust to the variation of  $\alpha$  value. This can be attributed to the following reason: The  $\alpha$  and  $\beta$  encapsulates different aspects of dark energy component namely its self interacting potential and its coupling with dark matter respectively, and hence are independent of each other.

The above points further supports the discussion in the

previous paragraphs which hinted towards the possible existence of a fifth force within the dark sector. Further, we can note that the mean values of  $H_0$ ,  $\sigma_8$  and  $\omega_{dm}$  seems to increase with the  $\alpha$  value.

We can note that since the Chameleon interaction has no effect on the CMB primary anisotropies (as described in Sec.III), the constraint obtained on the parameter  $\beta$  from the Planck dataset can be entirely credited to be coming from the CMB secondary anisotropies only, which originates at later times after the recombination era.

The BAO, Pantheon Plus, and SH<sub>0</sub>ES datasets capture

information about the physics in the late-time evolution of the Universe i.e. at specific low redshift or at a range of low redshifts. And further the Chameleon model also starts to significantly alter the evolution at later times. Hence adding these late-time observational datasets to Planck dataset leads to a better and better shaped posterior distributions of  $\beta$ . Further, as noted earlier the likelihood value at  $\beta = 0$  decreases with the consecutive addition of each of these datasets which in turn implies that the non-interacting dark energy scenario is becoming less and less probable in these consecutive cases respectively even though it cannot be ruled out entirely.

The analysis and discussions so far point towards a mild detection of fifth force within the dark sector, which perhaps can be attributed to the following significant improvements in the current work: i) The use of exact solution obtained by numerically solving the modified Klein-Gordan equation in Eq. 1 using the shooting method, which was then solved together with the background and perturbation equations of Chameleon model with the CLASS package. ii) The use of latest cosmological datasets for the MCMC analysis.

In Desmond et. al. [102], they constrain the relative strength of a fifth force arising from a Yukawa type Chameleon scalar field, for screened and un-screened cases, using the ALFALFA survey of neutral atomic hydrogen. They quantify the relative strength as  $\Delta G/G_N$ , where  $G_N$  is the Newtonian gravitational constant,  $\Delta G$  is the strength of new interaction relative to gravitational force. They found an evidence of  $6.6\sigma$  for  $\Delta G > 0$  at  $\lambda_c = 2\text{Mpc}$  with  $\Delta G/G_N = 0.025$  for the case with screening. While for the no-screening case, they found no increase in the likelihood over the case with  $\Delta G = 0$  for any  $\lambda_c$ . They mention that they could not rule out the possibility that this detection could have originated from other effects such as the galaxy formation physics. Hence they show a more conservative results which yields only upper limits on  $\Delta G/G_N$  ranging from  $\sim 10^{-1}$  for  $\lambda_c \simeq 0.5\text{Mpc}$  to  $\sim \text{few} \times 10^{-4}$  at  $\lambda_c \simeq 50\text{Mpc}$ .

We can compare our results with Desmond et. al. [102], since the parameter  $\beta$  is related to the relative strength as  $\Delta G/G_N = 2\beta^2$  (from Eq.6). The relative strength can then be estimated for the Chameleon model corresponding to the different dataset combinations of Planck, BAO, Pantheon Plus, and SH<sub>0</sub>ES, in tandem with the inclusion of each dataset, to be 0.0052, 0.0057, 0.0054, 0.0087 respectively (using the mean value of  $\beta$  posterior distribution). Further, the corresponding fifth force range now is approximately equal to the current size of the observable Universe (from Eq.7) implying that the fifth force in the Chameleon model becomes a long range force at the later times. We can note that our estimates of fifth force relative strength are consistent with their conservative estimate at  $\lambda_c \simeq 0.5\text{Mpc}$  while it is about an order of magnitude higher in comparison to their conservative estimate at  $\lambda_c \simeq 50\text{Mpc}$ . This difference can be attributed to the different approaches adopted which are listed as follows: i) They consider

the fifth force to originate from the coupling of screened scalar field with the stars, gas and dark matter while in our work we consider the fifth force to originate from the dark energy which is assumed to couple with only the dark matter. ii) Our estimates use cosmological datasets while their analysis is based on searching for displacements between galaxies stellar and gas mass centroids in galaxy surveys. iii) While our study focuses on the impact of fifth force at cosmological scales, their study focus on scales of  $0.4 - 50\text{Mpc}$ . In conclusion irrespective of the different approaches adopted in these works, both offer intriguing and complementary hints towards the existence of a fifth force.

## V. CONCLUSION

We have investigated the Yukawa-type interaction between the dark energy and dark matter arising in the Chameleon model. The associated background and perturbation equations were numerically solved using the shooting algorithm. A thorough analysis was then conducted using the MCMC method. The main findings of this analysis are as follows:

- ▶ The strength of dark sector interaction, obtained from the peak of posterior distribution of  $\beta$ , for different dataset combinations of Planck, BAO, Pantheon Plus, and SH<sub>0</sub>ES in tandem with the inclusion of each dataset are 0.0512, 0.0537, 0.0520, 0.0660 respectively. The corresponding bestfit values are 0.0487, 0.0680, 0.0712, 0.0822 respectively.
- ▶ The  $\Delta\chi^2_{min}$  values obtained for the Chameleon model, with the additional parameter  $\beta$ , relative to the  $\Lambda\text{CDM}$  model does not indicate a very significant preference but still all of the different dataset combinations consistently shows a slight but definite preference.
- ▶ The different dataset combinations show higher likelihood for non-zero  $\beta$  value in comparison to that of  $\beta = 0$  (which refers to non-interacting dark sector). This indicates that the cosmological datasets are hinting at an interacting dark sector.
- ▶ The strength of the fifth force with respect to the gravitational force,  $\Delta G/G_N$ , due to the Chameleon dark energy was estimated corresponding to the different dataset combinations of Planck, BAO, Pantheon Plus, and SH<sub>0</sub>ES in tandem with the inclusion of each dataset as 0.0052, 0.0057, 0.0054, 0.0087 respectively.

This mild detection of fifth force within the dark sector which perhaps could have resulted because we use the exact solution, obtained by numerically solving the modified Klein-Gordan equation using the shooting method,



and the use of latest cosmological datasets for the MCMC analysis.

The hints of a non-zero value for  $\beta$  being favored by the analysis of linear scales motivate extending the analysis to smaller, more nonlinear scales. Differences in the linear  $P(k)$  on scales of  $k > 10^{-1}h/\text{Mpc}$  at  $z = 0$ , as seen in Fig. 1, should also translate to differences in the observable, nonlinear  $P(k)$  which will be measured with great precision in the various Stage IV cosmological surveys in the next decade. Given the statistical power on smaller scales (due to the number of independent modes), we expect to be able to either detect a non-zero  $\beta$  with much greater significance or constrain  $\beta$  much more stringently. There will also be unique signatures of a non-zero  $\beta$  value arising from the difference in the infall of Dark Matter and baryonic matter onto

virialized halos [77–79]. Numerical  $N$ -body simulations will be needed to quantify these effects accurately, where the usual  $N$ -body methods will need to be updated to correctly account for the Chameleon interactions, as well as differences in the forces on Dark Matter vs baryons. This will be part of a future study.

## ACKNOWLEDGMENTS

SD and VG acknowledge the DST-SERB Government of India grant CRG/2019/006147 for supporting the project. We acknowledge the use of NOVA, the high performance computing cluster situated at Indian Institute of Astrophysics, Bangalore where all of the numerical calculations in this paper was performed.

- 
- [1] N. Aghanim, Y. Akrami, M. Ashdown, and et. al. (Planck Collaboration), *Astronomy & Astrophysics* **641**, A6 (2020).
  - [2] A. Semenaite, A. G. Sánchez, A. Pezzotta, and et. al., *Monthly Notices of the Royal Astronomical Society* **512**, 5657 (2022), arXiv:2111.03156 [astro-ph.CO].
  - [3] I. Sevilla-Noarbe, K. Bechtol, M. Carrasco Kind, and et. al., *The Astrophysical Journal Supplement Series* **254**, 24 (2021).
  - [4] R. Dalal, X. Li, A. Nicola, and et. al., *Phys. Rev. D* **108**, 123519 (2023).
  - [5] X. Li, T. Zhang, S. Sugiyama, and et. al., *Phys. Rev. D* **108**, 123518 (2023).
  - [6] W. L. Freedman, *Nature Astronomy* **1**, 0121 (2017).
  - [7] C. Heymans, E. Grocutt, A. Heavens, and et. al., *Monthly Notices of the Royal Astronomical Society* **432**, 2433 (2013).
  - [8] S. Weinberg, *Rev. Mod. Phys.* **61**, 1 (1989).
  - [9] R. R. Caldwell, R. Dave, and P. J. Steinhardt, *Phys. Rev. Lett.* **80**, 1582 (1998).
  - [10] A. R. Liddle and R. J. Scherrer, *Phys. Rev. D* **59**, 023509 (1998).
  - [11] R. K. Sharma, K. L. Pandey, and S. Das, *The Astrophysical Journal* **934**, 113 (2022).
  - [12] A. G. Adame *et al.* (DESI), (2024), arXiv:2404.03002 [astro-ph.CO].
  - [13] C. Wetterich, *Nuclear Physics B* **302**, 668 (1988).
  - [14] C. Wetterich, *Astronomy & Astrophysics* **301**, 321 (1995), arXiv:hep-th/9408025 [hep-th].
  - [15] T. Damour, G. W. Gibbons, and C. Gundlach, *Phys. Rev. Lett.* **64**, 123 (1990).
  - [16] J. A. Casas, J. Garcia-Bellido, and M. Quiros, *Classical and Quantum Gravity* **9**, 1371–1384 (1992).
  - [17] G. W. Anderson and S. M. Carroll, in *COSMO-97* (WORLD SCIENTIFIC, 1998).
  - [18] L. Amendola, *Phys. Rev. D* **62**, 043511 (2000).
  - [19] L. Amendola and D. Tocchini-Valentini, *Phys. Rev. D* **64**, 043509 (2001).
  - [20] R. Bean, *Phys. Rev. D* **64**, 123516 (2001).
  - [21] T. Damour, F. Piazza, and G. Veneziano, *Phys. Rev. Lett.* **89**, 081601 (2002).
  - [22] D. Comelli, M. Pietroni, and A. Riotto, *Physics Letters B* **571**, 115–120 (2003).
  - [23] L. Amendola, C. Quercellini, D. Tocchini-Valentini, and A. Pasqui, *The Astrophysical Journal* **583**, L53 (2003).
  - [24] L. P. Chimento, A. S. Jakubi, D. Pavón, and W. Zimdahl, *Phys. Rev. D* **67**, 083513 (2003).
  - [25] L. Amendola and C. Quercellini, *Phys. Rev. D* **68**, 023514 (2003).
  - [26] U. França and R. Rosenfeld, *Phys. Rev. D* **69**, 063517 (2004).
  - [27] J. Khoury and A. Weltman, *Phys. Rev. Lett.* **93**, 171104 (2004).
  - [28] J. Khoury and A. Weltman, *Phys. Rev. D* **69**, 044026 (2004).
  - [29] P. Brax, C. van de Bruck, A.-C. Davis, and et. al., *Phys. Rev. D* **70**, 123518 (2004).
  - [30] G. R. Farrar and P. J. E. Peebles, *The Astrophysical Journal* **604**, 1–11 (2004).
  - [31] S. S. Gubser and J. Khoury, *Physical Review D* **70** (2004).
  - [32] D. B. Kaplan, A. E. Nelson, and N. Weiner, *Phys. Rev. Lett.* **93**, 091801 (2004).
  - [33] G. Olivares, F. Atrio-Barandela, and D. Pavón, *Physical Review D* **71** (2005).
  - [34] H. Wei and R.-G. Cai, *Phys. Rev. D* **71**, 043504 (2005).
  - [35] R. D. Peccei, *Physical Review D* **71** (2005).
  - [36] R. Fardon, A. E. Nelson, and N. Weiner, *Journal of High Energy Physics* **2006**, 042–042 (2006).
  - [37] R. von Martens, L. Lombriser, M. Kunz, and et. al., *Physics of the Dark Universe* **28**, 100490 (2020).
  - [38] O. Baker, A. Afanasev, T. Lagouri, and et. al., *Symmetry* **14**, 2238 (2022).
  - [39] H.-C. Zhang, (2022), arXiv:2210.10204 [gr-qc].
  - [40] E. Piedipalumbo, S. Vignolo, P. Feola, and S. Capozziello, *Phys. Dark Univ.* **42**, 101274 (2023), arXiv:2307.02355 [gr-qc].
  - [41] P. Brax, C. P. Burgess, and F. Quevedo, *JCAP* **03**, 015, arXiv:2310.02092 [hep-th].
  - [42] C. Käding, M. Pitschmann, and C. Voith, *Eur. Phys. J. C* **83**, 767 (2023), arXiv:2306.10896 [hep-ph].
  - [43] A. Singh, A. Pradhan, and A. Beesham, *New Astron.* **100**, 101995 (2023).
  - [44] C. Burgess and F. Quevedo, *Journal of Cosmology and*

- Astroparticle Physics* **2022** (04), 007.
- [45] P. Brax, C. P. Burgess, and F. Quevedo, *JCAP* **08**, 011, [arXiv:2212.14870 \[hep-ph\]](#).
- [46] M. A. van der Westhuizen and A. Abebe, *Journal of Cosmology and Astroparticle Physics* **2024** (01), 048.
- [47] E. Di Valentino, A. Melchiorri, O. Mena, and S. Vagnozzi, *Physics of the Dark Universe* **30**, 100666 (2020).
- [48] Y. L. Bolotin, A. Kostenko, O. A. Lemets, and D. A. Yerokhin, *Int. J. Mod. Phys. D* **24**, 1530007 (2014), [arXiv:1310.0085 \[astro-ph.CO\]](#).
- [49] S. Pan, J. de Haro, W. Yang, and J. Amorós, *Phys. Rev. D* **101**, 123506 (2020).
- [50] M. Lucca and D. C. Hooper, *Phys. Rev. D* **102**, 123502 (2020).
- [51] E. Di Valentino, A. Melchiorri, O. Mena, and S. Vagnozzi, *Phys. Rev. D* **101**, 063502 (2020).
- [52] E. Di Valentino, A. Melchiorri, O. Mena, S. Pan, and W. Yang, *Monthly Notices of the Royal Astronomical Society: Letters* **502**, L23 (2021), <https://academic.oup.com/mnras/article-pdf/502/1/L23/54638399/slaa207.pdf>.
- [53] Y. Liu, S. Liao, X. Liu, J. Zhang, R. An, and Z. Fan, *Monthly Notices of the Royal Astronomical Society* **511**, 3076 (2022), <https://academic.oup.com/mnras/article-pdf/511/2/3076/42541181/stac229.pdf>.
- [54] C. Li, X. Ren, M. Khurshudyan, and Y.-F. Cai, *Physics Letters B* **801**, 135141 (2020).
- [55] R. R. Bachega, A. A. Costa, E. Abdalla, and K. Fornazier, *Journal of Cosmology and Astroparticle Physics* **2020** (05), 021.
- [56] H.-L. Li, D.-Z. He, J.-F. Zhang, and X. Zhang, *Journal of Cosmology and Astroparticle Physics* **2020** (06), 038.
- [57] U. Mukhopadhyay, A. Paul, and D. Majumdar, *Eur. Phys. J. C* **80**, 904 (2020), [arXiv:1909.03925 \[astro-ph.CO\]](#).
- [58] R. von Marttens, H. A. Borges, S. Carneiro, J. S. Alcaniz, and W. Zimdahl, *Eur. Phys. J. C* **80**, 1110 (2020), [arXiv:1909.10336 \[gr-qc\]](#).
- [59] R. Kase and S. Tsujikawa, *Phys. Rev. D* **101**, 063511 (2020).
- [60] X.-W. Liu, C. Heneka, and L. Amendola, *Journal of Cosmology and Astroparticle Physics* **2020** (05), 038.
- [61] R. Kase and S. Tsujikawa, *Physics Letters B* **804**, 135400 (2020).
- [62] F. N. Chamings, A. Avgoustidis, E. J. Copeland, A. M. Green, and A. Pourtsidou, *Phys. Rev. D* **101**, 043531 (2020).
- [63] D. Benisty, E. I. Guendelman, E. Nissimov, and S. Pacheva, *Symmetry* **12**, 10.3390/sym12030481 (2020).
- [64] L. Amendola and S. Tsujikawa, *Journal of Cosmology and Astroparticle Physics* **2020** (06), 020.
- [65] D. Benisty, E. I. Guendelman, E. Nissimov, and S. Pacheva, *Int. J. Mod. Phys. D* **26**, 2050104 (2020), [arXiv:2003.13146 \[astro-ph.CO\]](#).
- [66] W. Yang, S. Pan, R. C. Nunes, and D. F. Mota, *Journal of Cosmology and Astroparticle Physics* **2020** (04), 008.
- [67] J. D. Barrow and G. Kittou, *Eur. Phys. J. C* **80**, 120 (2020), [arXiv:1907.06410 \[gr-qc\]](#).
- [68] E. Silva, U. Zúñiga Bolaño, R. C. Nunes, and E. Di Valentino, (2024), [arXiv:2403.19590 \[astro-ph.CO\]](#).
- [69] P. Shah, G. C. Samanta, K. Bamba, and R. Myrzakulov, *Int. J. Geom. Meth. Mod. Phys.* **20**, 2350042 (2023), [arXiv:2403.08263 \[gr-qc\]](#).
- [70] J. S. T. de Souza, G. S. Vicente, and L. L. Graef, (2024), [arXiv:2403.04970 \[astro-ph.CO\]](#).
- [71] S. Halder, J. de Haro, T. Saha, and S. Pan, (2024), [arXiv:2403.01397 \[gr-qc\]](#).
- [72] G. Huey and B. D. Wandelt, *Physical Review D* **74** (2006).
- [73] H. Štefančić, *The European Physical Journal C* **36**, 523–527 (2004).
- [74] S. Das, P. S. Corasaniti, and J. Khoury, *Phys. Rev. D* **73**, 083509 (2006).
- [75] T. Damour and A. Polyakov, *Nuclear Physics B* **423**, 532–558 (1994).
- [76] D. Boriero, S. Das, and Y. Y. Wong, *Journal of Cosmology and Astroparticle Physics* **2015** (07), 033.
- [77] M. Kesden and M. Kamionkowski, *Physical Review D* **74**, 083007 (2006).
- [78] J. A. Keselman, A. Nusser, and P. J. E. Peebles, *Physical Review D* **80** (2009).
- [79] L. F. Secco, A. Farah, B. Jain, and et. al., *The Astrophysical Journal* **860**, 32 (2018).
- [80] P. Brax, C. van de Bruck, A. Davis, and A. Green, *Physics Letters B* **633**, 441 (2006).
- [81] E. J. Copeland, M. Sami, and S. Tsujikawa, *International Journal of Modern Physics D* **15**, 1753–1935 (2006).
- [82] J. Wang, L. Hui, and J. Khoury, *Phys. Rev. Lett.* **109**, 241301 (2012).
- [83] C. M. Will, *Living Reviews in Relativity* **4** (2001).
- [84] D. J. Kapner, T. S. Cook, E. G. Adelberger, and et. al., *Phys. Rev. Lett.* **98**, 021101 (2007).
- [85] S. Alam, M. Aubert, S. Avila, and et. al., *Phys. Rev. D* **103**, 083533 (2021).
- [86] G. D’Amico, L. Senatore, and P. Zhang, *Journal of Cosmology and Astroparticle Physics* **2021** (01), 006.
- [87] T. M. C. Abbott, F. B. Abdalla, S. Avila, and et. al. (DES Collaboration), *Phys. Rev. D* **99**, 123505 (2019).
- [88] P. S. Corasaniti, *Phys. Rev. D* **78**, 083538 (2008).
- [89] T. Abbott, F. B. Abdalla, A. Alarcon, and et. al., *Physical Review D* **98** (2018).
- [90] P. Brax, C. van de Bruck, A. C. Davis, and et. al., *AIP Conference Proceedings* **736**, 105 (2004).
- [91] J. Lesgourgues, (2011), [arXiv:1104.2932 \[astro-ph.IM\]](#).
- [92] D. Blas, J. Lesgourgues, and T. Tram, *Journal of Cosmology and Astroparticle Physics* **2011** (07), 034.
- [93] Aghanim, N., Akrami, Y., Ashdown, M., and et. al. (Planck Collaboration), *A&A* **641**, A5 (2020).
- [94] S. Alam, M. Ata, S. Bailey, and et. al., *Monthly Notices of the Royal Astronomical Society* **470**, 2617–2652 (2017).
- [95] F. Beutler, C. Blake, M. Colless, and et. al., *Monthly Notices of the Royal Astronomical Society* **416**, 3017–3032 (2011).
- [96] A. J. Ross, L. Samushia, C. Howlett, and et. al., *Monthly Notices of the Royal Astronomical Society* **449**, 835–847 (2015).
- [97] D. Brout, D. Scolnic, B. Popovic, and et. al., *The Astrophysical Journal* **938**, 110 (2022).
- [98] A. G. Riess, W. Yuan, L. M. Macri, and et. al., *The Astrophysical Journal Letters* **934**, L7 (2022).
- [99] T. Brinckmann and J. Lesgourgues, (2018), [arXiv:1804.07261 \[astro-ph.CO\]](#).
- [100] A. Lewis, A. Challinor, and A. Lasenby, *The Astrophys-*

- ical Journal **538**, 473 (2000).
- [101] A. Gelman and D. B. Rubin, *Statistical Science* **7**, 457 (1992).
- [102] H. Desmond, P. G. Ferreira, G. Lavaux, and J. Jasche, *Phys. Rev. D* **98**, 064015 (2018).

### Appendix A: $\chi^2$ per experiment

We report the bestfit  $\chi^2$  values per experiment for the  $\Lambda$ CDM and Chameleon model corresponding to different dataset combinations in Table III.

We note from the table that the bestfit  $\chi^2$  values of Planck high- $\ell$ , Pantheon Plus and SH<sub>0</sub>ES datasets seems

to show a preference to Chameleon model. While the Planck low- $\ell$  TT, Planck low- $\ell$  EE, BAO BOSS DR12 and BAO low  $z$  datasets either does not show preference or shows a comparatively smaller preference to the Chameleon model. The behaviour noted in the case of Planck low- $\ell$  datasets can be interpreted as follows: The Planck low- $\ell$  TT and EE datasets corresponds to large Cosmic Microwave Background perturbation scales ( $\ell < 30$ ) that originated at early times but has mostly remained unaltered due to the later evolution. Hence it supports the standard  $\Lambda$ CDM model over the Chameleon model, which as previously noted significantly alters the evolution only at later times.

Dataset Combination $\rightarrow$		D1		D2		D3		D4	
Experiment $\downarrow$	Model $\rightarrow$	$\Lambda$ CDM	Chameleon	$\Lambda$ CDM	Chameleon	$\Lambda$ CDM	Chameleon	$\Lambda$ CDM	Chameleon
Planck high- $\ell$	TTTEEE	2351.5205	2348.4028	2353.1730	2348.7670	2353.4624	2350.9443	2357.8959	2355.9107
Planck low- $\ell$	EE	396.7873	397.3647	395.7295	397.2702	395.7135	395.7490	396.4642	396.1857
Planck low- $\ell$	TT	23.4834	25.3441	22.7220	24.8302	23.3171	24.6166	21.9501	24.4752
BAO BOSS DR12		–	–	4.1515	3.5268	4.0200	6.7074	3.4827	3.6519
BAO low z		–	–	1.2996	1.6461	1.3488	0.8624	2.2277	2.3994
Pantheon Plus		–	–	–	–	1411.6825	1410.4646	–	–
Pantheon Plus+SH <sub>0</sub> ES		–	–	–	–	–	–	1322.1737	1318.6652
Total $\chi^2_{min}$		2771.7913	2771.1117	2777.0758	2776.0405	4189.5447	4189.3447	4104.1945	4101.2884
$\Delta\chi^2_{min}$ (Chameleon - $\Lambda$ CDM)		0	-0.6796	0	-1.0353	0	-0.2000	0	-2.9061

TABLE III. The bestfit  $\chi^2$  per experiment for  $\Lambda$ CDM and Chameleon model corresponding to different dataset combinations namely D1, D2, D3, and D4 (where D1  $\equiv$  Planck, D2  $\equiv$  D1 + BAO, D3  $\equiv$  D2 + Pantheon Plus and D4  $\equiv$  D2 + Pantheon Plus + SH<sub>0</sub>ES). The total  $\chi^2_{min}$  and  $\Delta\chi^2_{min}$  are shown in the last rows.